SPE-191818-18ERM-MS

Estimation of Fracability of the Marcellus Shale: A Case Study from the MIP3H in Monongalia County, West Virginia, USA

Yixuan Zhu and Timothy R. Carr, West Virginia University

This paper was prepared for presentation at the SPE Eastern Regional Meeting held in Pittsburgh, Pennsylvania, USA, 7 - 11 October 2018.

Abstract

Hydraulic fracturing is critical to economic production of shale oil and gas from unconventional reservoirs. Success of completion is closely related to gas production. The brittleness index is widely used as a measurement of ability of hydraulic fracturing. However, the index may not be a unique and explicit indicator for estimating "fracability". In the Marcellus Shale of our study area, there is discrepancy between brittleness index calculated from mineralogy and that from elastic moduli. In addition, the brittleness index does not explain why the large majority of microseismic events were generated well above the Marcellus Shale. Two other factors appear to control fracture stimulation. One is the presence of pre-existing natural fractures. Natural fractures, measured and interpreted from the FMI log, show that fractures developed in similar patterns with high dip angle in the Marcellus and overlying Mahantango shale units, which are favorable for vertical fracture propagation. The other factor is geomechanical characterization. The Marcellus Shale has obvious presence of overpressure. According to the study on stress state using a Mohr's circle, overpressure in the Marcellus Shale increases the possibility of frictional sliding of pre-existing fractures especially at lower value of least principal stress, and will keep some fractures at certain dip angles open, although some of them are in non-active state. Unconfined compressive strength (UCS) is used to estimate rock strength in overpressure strata. The result calculated from empirical equations shows that the Marcellus Shale has significantly lower rock strength, which continues up into the Mahantango Formation, and explain vertical hydraulic fracture growth.

Introduction

To optimize hydraulic fracturing, completion quality is an important factor to maximize shale gas production. In recent years, brittleness has been widely used in industry to evaluate the ability to hydraulic fracture a shale gas reservoir. Brittleness has been estimated using data either from lab analysis or from well logging. Jarvie *et al*. (2007) reported that a high amount of quartz is an indication of brittleness in terms of mineral components. Wang *et al*. (2009) believed that dolomite should also be considered as brittle part in addition to quartz, while organic matter would increase ductility. In addition to the study of brittle mineral components, characteristics of elastic moduli are also used to distinguish brittle and ductile shale. Richman *et al*. (2008) indicated that brittle rock has higher Young's modulus and lower Poisson's ratio, and

considered brittleness as an average of normalized Young's modulus and Poisson's ratio. In our study area, the brittleness index calculated from minerals is not in accordance with that calculated from elastic moduli.

The wells are located in Monongalia County, West Virginia and are part of the Marcellus Energy and Environment Lab (MSEEL) (Figure 1). In the study area, the Marcellus Shale is buried at a depth of approximately 7500 ft (2286 m). Two horizontal wells drilled toward the northwest were monitored and logged with microseismic and fiber-optic distributed acoustic sensing (DAS) and distributed temperature sensing (DTS) (Figure 2). The vertical pilot hole of the MIP3H is used to compute the brittleness index (Figure 3). Brittleness indexes calculated from Jarvie *et al*. (2007) and Wang *et al*. (2009) show nearly identical trends. Shale units of the Marcellus Shale and Mahantango Formation are more brittle than limestone units of the overlying Tully Limestone and underlying Onondaga Limestone. On the contrary, the brittleness in terms of elastic moduli shows higher values on the Tully and Onondaga limestone units, while the Marcellus Shale is more ductile. This contrast between mineralogical brittleness and brittleness measured from elastic moduli does not provide an explicit characterization of brittleness.

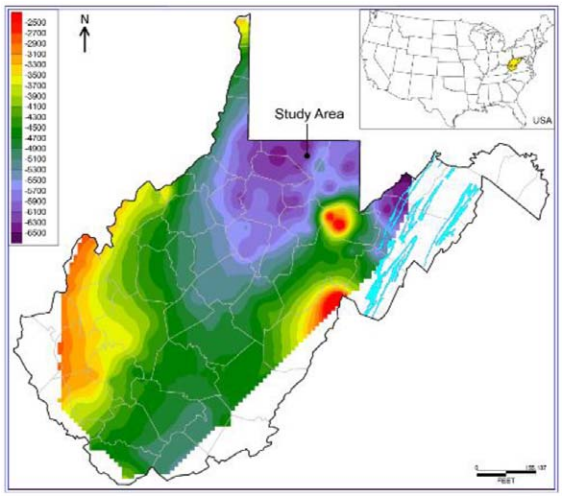

Figure 1—Structural map of subsea burial depth of the Marcellus Shale in West Virginia, USA, showing location of the wells used in this study.

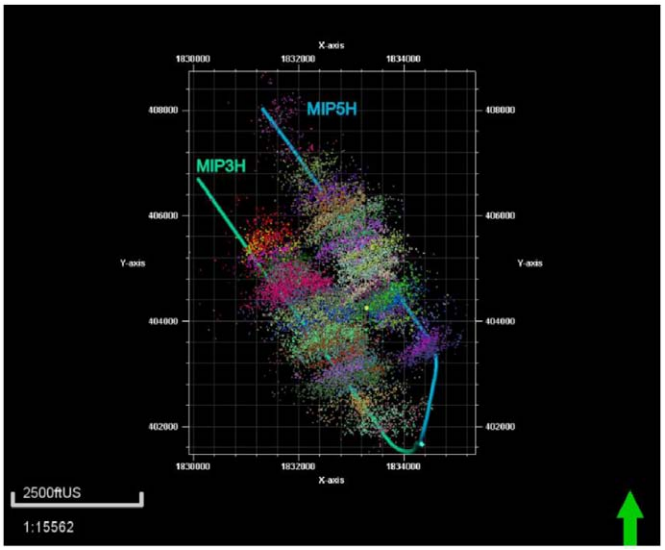

Figure 2—Map view of two horizontal wells at the Marcellus Shale Energy and Environment Lab (MSEEL) with microseismic events recorded during stimulation of the MIP3H and MIP5H.

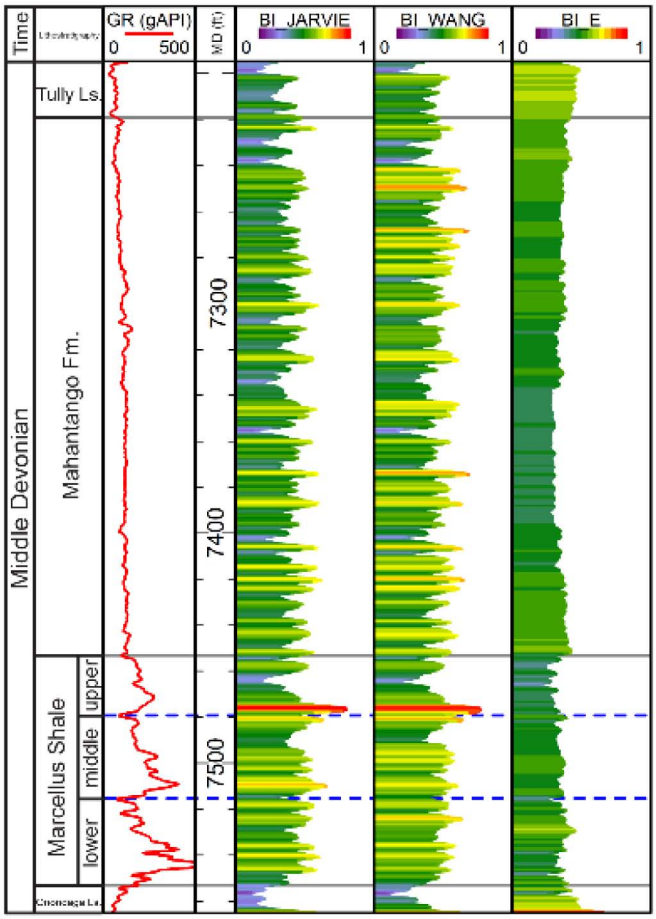

Figure 3—Brittleness index calculated for the MIP3H pilot hole from the Tully Limestone to the Onondaga Limestone adopting methods from Jarvie et al. (2007) (BI_JARVIE, Track 2), Wang et al. (2009) (BI_WANG, Track 3), and elastic moduli following Richman et al. (2008) (BI_E, Track 4). Gamma ray log is shown in Track 1.

Based on observation of microseismic data in study area, most of events are well above the top of the Marcellus Shale with the center of radiated microseismic energy located 160 ft (49 m) above the perforation clusters (Wilson *et al*. 2018). Dependent on the well, microseismic events located within the Marcellus Shale reservoir are 20% for the MIP3H and 15.8% for the MIP5H. For both horizontal wells, the majority of microseismic events fall into the overlying formations (Figure 4). For the MIP3H, a large number of events occur in the Mahantango Formation, which is characterized by organic-lean shale. For the MIP5H, most of events are located above the Tully Limestone and in the Mahantango Formation. In order to explore the factors that influence fracturing and result in microseismic events, the presence of pre-existing natural fractures and reservoir geomechanical characterization are examined using data from the MIP3H.

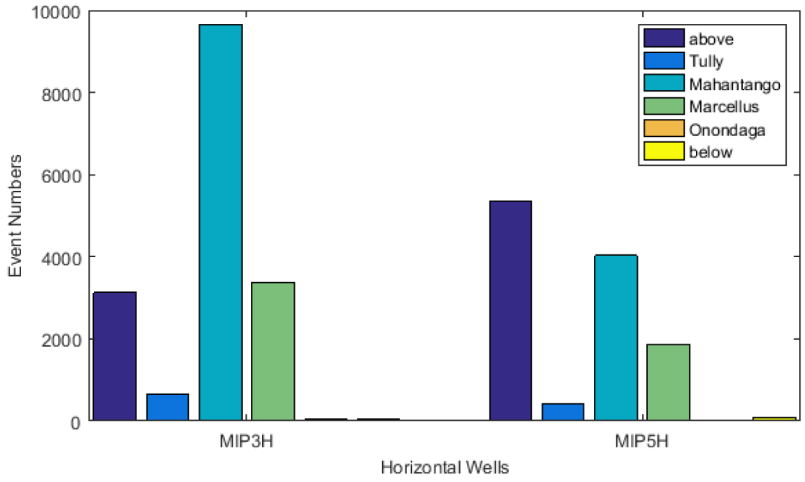

Figure 4—Histogram of microseismic events by stratigraphic unit for all stages of the MIP3H and MIP5H. The majority of microseismic events occur in stratigraphic units above the Marcellus Shale.

Natural Fractures and Fracture Density

FMI (full-bore formation microimager) logging was conducted for the vertical pilot hole of the MIP3H to detect fractures. From the Tully Limestone to the Onondaga Limestone, 71 fractures were identified. P32 fracture density, which is area of fracture over the volume, is plotted with stereonets in Figure 5. Stereonets show fractures orientation and dip for different depth ranges. In the Onondaga Limestone, no fractures were observed. For the Marcellus Shale, most fractures have a high dip angle (nearly vertical) with a dominant east-northeast strike (N87E for healed fractures). Based on P32 fracture density plot, the highest density of fractures is located at the middle part of the upper Marcellus, and fractures are distributed almost evenly through the middle Marcellus. Fractures were not observed at the carbonate separating the middle and lower Marcellus. A significant number of fractures were also not observed in the lowest parts of the Marcellus. For the Mahantango Formation, fractures developed similar to the Marcellus at a very high dip angle with dominant east-northeast direction. At the bottom of the Mahantango, the P32 log indicates that fractures are persistent across the contact with the Marcellus Shale. Fractures gradually decrease in the upper Mahantango Formation approaching the Tully Limestone. For the Tully Limestone, only three fractures appeared with middle to high dip angle and northeast strike.

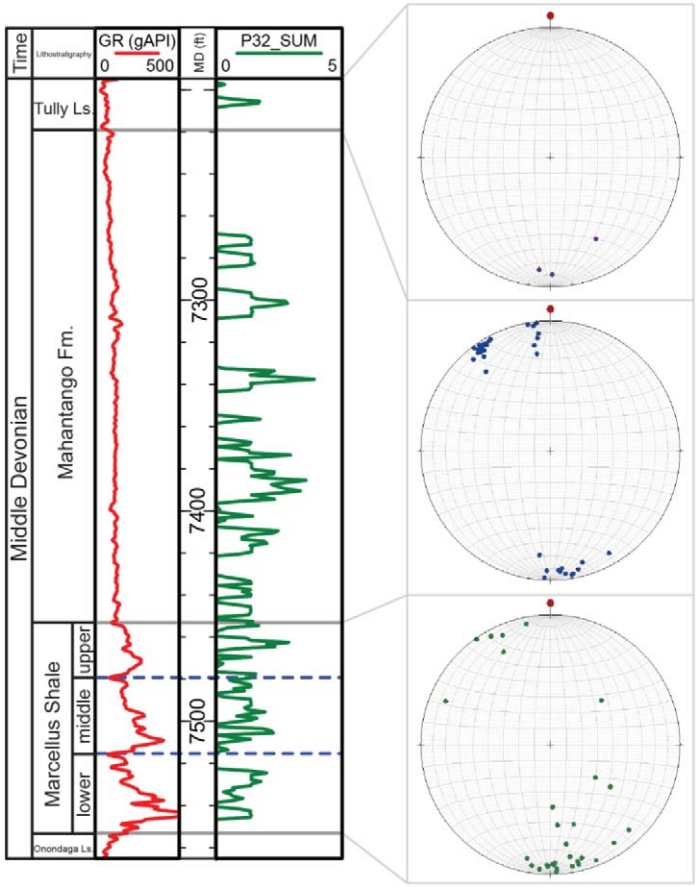

Figure 5—Fracture density P32 for the MIP3H pilot hole along with stereonets for fractures in the different ranges of the Tully Limestone, Mahantango Formation and Marcellus Shale.

Based on the FMI observations, fractures developed with similar orientation and high dip angle in the two shale units of the Marcellus and Mahantango. These fractures may be continuous or could be easily connected when they are activated during hydraulic fracturing, which may result in activation of fracture in the Marcellus Shale and moving up to the Mahantango Formation.

Geomechanical Characterization

Hydraulic fracturing involves both processes of breaking the rock matrix and activating pre-existing fractures in the subsurface. These two processes are closely related with pore pressure in terms of effective stress law, which is expressed by difference between principal stress and pore pressure. A rock may be destabilized by increasing pore pressure in relation to failures (Fjar *et al*., 2008). Rock failure can be defined by a Mohr's circle and failure envelope. Increasing pore pressure will result in Mohr's circle moving left and increasing the chance to intercept with failure envelope. It means that failure may be generated or activated during process of increasing pore pressure.

Based on definition, pore pressure represents a hydraulic potential with regard to earth's surface, and it assumes that pores are interconnected. Therefore, in normal condition, the pore pressure at a certain depth is equal to hydrostatic pore pressure. If pore pressure is larger than hydrostatic pore pressure, the phenomenon is described as overpressure. On the contrary, less than hydrostatic pore pressure will be seen as under-pressure. To predict pore pressure, sonic and resistivity log data are commonly used (Hottmann and Johnson, 1965; Eaton, 1975; Bowers, 1995). The normal trend of sonic log should be interpreted as a steady increase of the compressional wave velocity with depth, while for resistivity log, the normal trend is expressed as resistivity increasing. The rationale behind these increases in sonic compressional velocity and resistivity

is closely related with decrease of porosity under compaction with depth. In the pilot hole of the MIP3H, well log curves of compressional wave velocity and resistivity are shown in Figure 6. A major turning point is around a depth 4600ft (1402m) for both curves. Below the point, velocity is deviated from the normal trend and decreases with depth, which is the characteristic of overpressure. Different from velocity curve, resistivity decreases with depth first and then increases at deeper depth below the turning point. One reason may be resistivity log is sensitive to hydrocarbons which could cause an increase of resistivity. Because of the hydrocarbon effect, resistivity curve is influenced by presence of hydrocarbons except of porosity. Therefore, sonic well log is used to predict pore pressure.

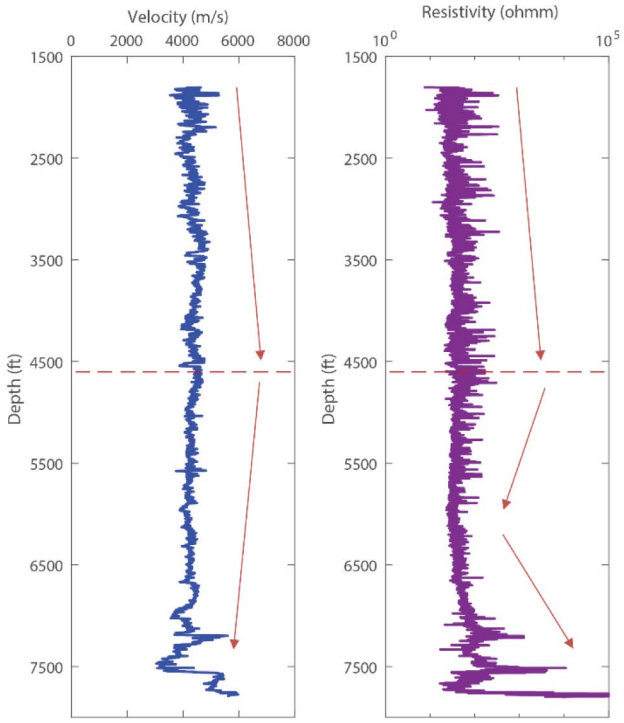

Figure 6—Variation trend of compressive wave velocity and resistivity well log curves in the pilot hole of the MIP3H.

A linear relationship exists between compressional wave velocity and depth, which velocity should increase with depth (Slotnick, 1936). Pore pressure is predicted using a method proposed by Eaton (1975), and adapted form in velocity shown as follow:

$$P_p = S_v - (S_v - P_h)\left(\frac{v_{\log}}{v_n}\right)^x, \quad (1)$$

where S_v is the vertical stress (psi); P_h is hydrostatic pore pressure (psi); v_{log} is sonic velocity of compressional wave from log data; v_n is sonic velocity of compressional wave from the normal trend; x is constant which is determined empirically. Mud weight in this well is used to constrain predicted pore pressure, because it serves as a role to balance pore pressure when drilling the well. In the condition of drilling in balance, it will reflect underground pore pressure in a certain degree. Therefore, calculated pore pressure should be close to pore pressure converted from mud weight. Based on this, exponent x is 1.0 for this well.

In the pilot hole of the MIP3H, predicted pore pressure is shown in Figure 7. Shale units of the Marcellus and Mahantango display the presence of overpressure. The overpressure increases the deviation of pore pressure from hydrostatic pressure and begins to approach vertical stress. It can be seen that effective stress is reduced from the expected normal trend. In the range from the Tully Limestone to the Onondaga Limestone,

the highest deviation of pore pressure is located at the Marcellus Shale (Figure 7c). Pore pressure for the Mahantango Formation is lower than that in the Marcellus Shale, but it increases with depth and approaches pore pressure of the Marcellus Shale at the contact of these two shale units. For the Tully Limestone and Onondaga Limestone, pore pressure drops to approximately hydrostatic pressure.

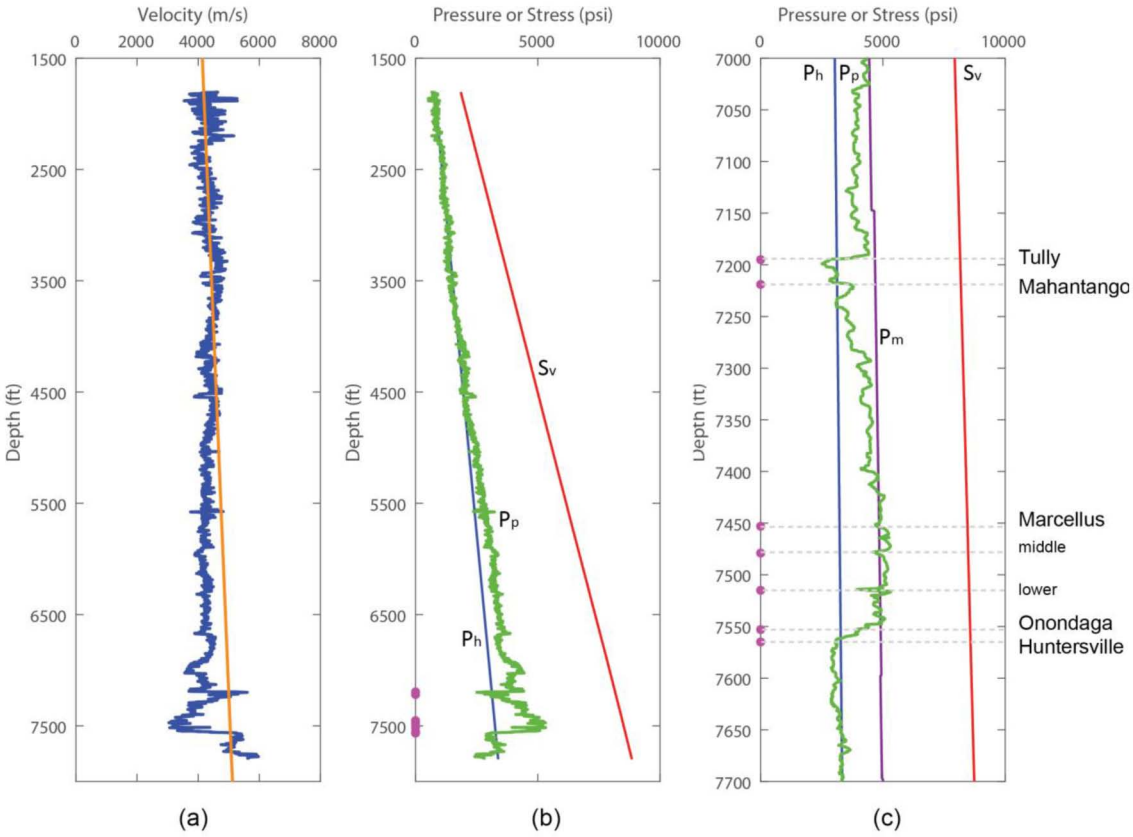

Figure 7—Pilot hole of the MIP3H showing (a) compressive wave velocity plotted with depth, (b) pore pressure calculated form compressional wave velocity, and (c) pore pressure (P_p) compared with pore pressure from mud weight (P_m), hydrostatic pressure (P_h) and vertical stress (S_v).

Activation of pre-existing open and healed fractures is one situation involved in hydraulic fracturing. Based on Amonton's law for frictional sliding, a fracture plane will be activated when the ratio of shear to normal stress approaches the coefficient of friction (μ). Dependent on the study of coefficient of friction on wide range of rocks, the lower bound value of 0.6 is used in this paper (Byerlee 1978).

In the MIP3H, values of minimum horizontal stress (S_{hmin}) are from instantaneous shut in pressure (ISIP) in hydraulic fracturing. There are total 21 ISIP recorded during hydraulic fracturing. Compared these S_{hmin} with corresponding values of S_v, it shows that all S_{hmin} are smaller than S_v. Therefore, the possible stress regime is normal or strike-slip faulting stress regime rather than reverse faulting stress regime. Assuming a normal faulting stress regime in study area, greatest principal stress (σ_1) will be equal to vertical stress (S_v), and least principal stress (σ_3) will be equal to minimum horizontal stress (S_{hmin}), according to Anderson's classification (1951) of style of faulting. In order to explore change of Mohr's circle corresponding to different least principal stress, values of maximum and minimum ISIP are chosen for evaluation. Mohr's circles expressed by effective stresses are plotted with coefficient of friction (Figure 8). The blue circle is calculated using minimum ISIP, whereas the green circle using maximum ISIP. Figures 8a and 8b represent different conditions. In normal or hydrostatic pore pressure condition (Figure 8a), both circles do not touch the frictional sliding line. It means that frictional sliding will not occur along pre-existing fractures. In the overpressure conditions observed in the Marcellus and Mahantango (Figure 8b), overpressure moves both

circles to left. The blue circle intercepts with frictional sliding line, but the green circle is still under the line in spite of overpressure. The position of the circle relative to frictional sliding line illustrates that pre-existing fractures have propensity to be activated. Activation is not only affected by pore pressure, but also dependent on magnitude of least principal stress (ISIP in this paper). Therefore, the activation of pre-existing fractures is location based, and should be considered stage by stage. The study result shows that under lower ISIP the Mohr's circle is more likely to touch the frictional sliding line. Moreover, the blue circle are intercepted the line with two points, and it implies that pre-existing fractures will be activated in the range with dip angle between 41.3° and 79.6°. In order to make comparison between stress state and fractures, assuming fractures in the range of the Marcellus Shale interpreted by FMI from the MIP3H pilot hole reflect the general condition in the study area, they are plotted onto the blue circle (Figure 8b). Orange points are conductive (open) fractures, and blue points are resistive (healed) fractures. In total 30 fractures, 13 fractures are located above sliding line on Mohr's circle including 3 conductive fractures, and 17 fractures are located below the sliding line. It suggests that some fractures are active fractures in the extreme condition of minimum value of ISIP. In this condition, presence of overpressure in the Marcellus Shale may keep some fractures in certain dip angle open, although some of them are in a non-active state.

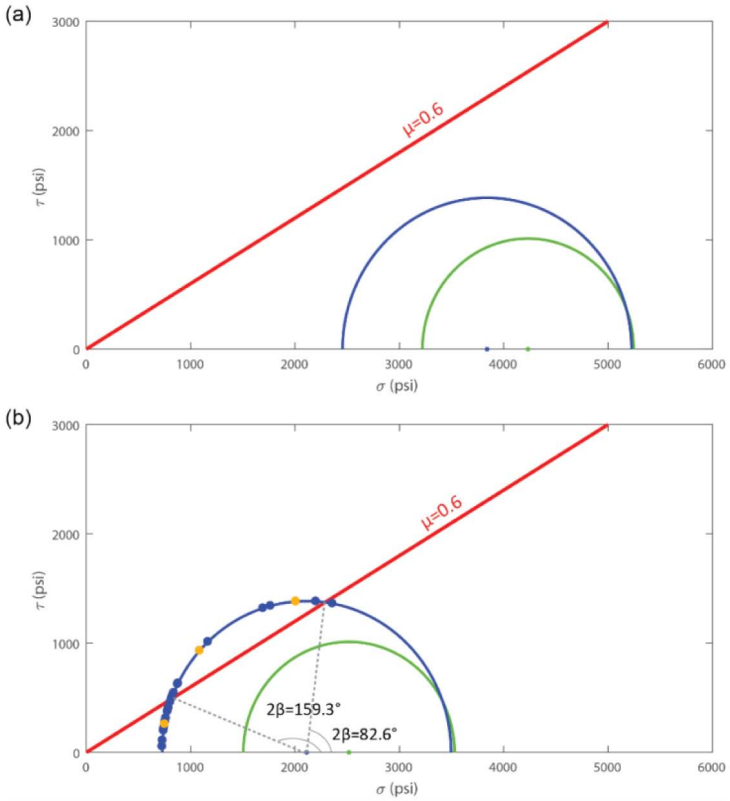

Figure 8—Mohr's circle with frictional sliding line showing (a) normal or hydrostatic conditions for the vertical depth of the MIP3H, and (b) overpressure condition in the well as computed from logs and mud weights. Blue Mohr's circle describes minimum effective stress state, while green circle represents maximum effective stress state. Points on the blue circle are fractures observed from FMI log. Orange points are conductive fractures, while blue points are resistive fractures.

In addition to activation of pre-existing fractures, another process is breaking rocks in hydraulic fracturing if rock matrix is treated as isotropic (i.e. without the influence of preferential zones of failure). Relating Mohr's circle, rock fracture is described by a failure envelope. A linearized Mohr envelope defined by two parameters in terms of normal and shear stress. The one is coefficient of internal friction; the other is cohesion. As cohesion cannot be measured physically from experiments, unconfined compressive strength (UCS) is usually used to express rock strength. On Mohr's circle, UCS is expressed as value of σ_1, when σ_3

is equal to zero. In the case of the MIP3H, pore pressure in the shale units is higher than hydrostatic pore pressure, which results in Mohr's circle moving to the left and effective least principal stress approaching zero. In this situation, UCS could be used to reflect the "fracability" under overpressure conditions. In the MIP3H, UCS is calculated using the empirical equations for shale and limestone summarized by Zoback (2010) (Figure 9). UCS for limestone is used as a comparison and its "fracability" in the subsurface is subject to change as pore pressure drops to normal. The red curve is calculated based on relation with porosity, and shows a significant difference between the shale units and overlying and underlying limestone units. The blue curve relies on empirical relation to Young's modulus.

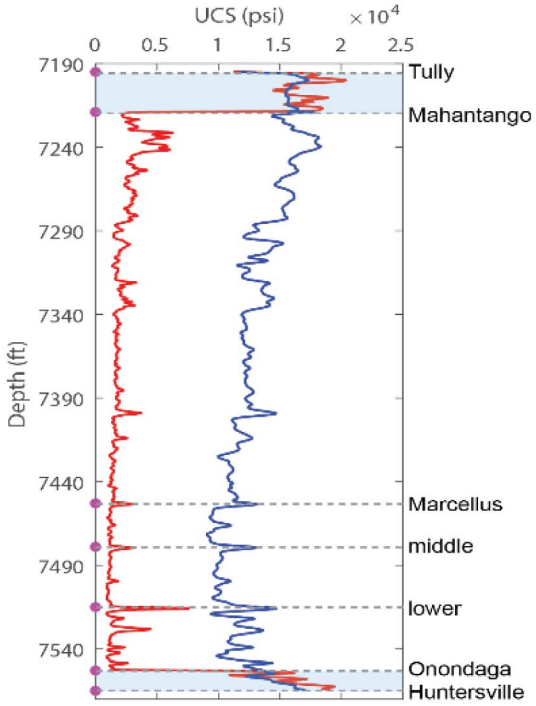

Figure 9—Prediction of rock strength for shale and limestone sections along with unit tops. Red curve is UCS calculated from empirical relation with porosity, while blue curve is computed from relation with Young's modulus. The blue block highlights the limestone units underlying and overlying the shale units.

The upper and middle Marcellus organic-rich shale units have the lowest strength, and the strength of lower organic-rich shale unit of the Marcellus is slightly higher. For the Mahantango Formation, rock strength is generally higher than the Marcellus with an upward increasing trend. It is worth noting that UCS of lower part of the Mahantango is close to that of the Marcellus at the boundary of these two units. Based on observations, it implies that the upper Marcellus and middle Marcellus are relatively easier to fracture, and given the similarity of UCS at the boundary of the Marcellus and Mahantango rock failure would be expected to grow upwards into the overlying units. This may explain the dominance of microseismic events above the Marcellus Shale.

Conclusions

Brittleness index may not be the unique and explicit index of "fracability". In our study area, it shows discrepancy between the brittleness indexes calculated from mineralogy and elastic moduli. Compared with microseismic data, brittleness index cannot provide an explicit explanation for distribution of microseismic events. In order to explain this phenomenon, two factors of "fracability" are proposed in this paper. The first one is pre-existing natural fractures. Fractures are developed in similar patterns with high dip angle in the two shale units of the Marcellus and Mahantango. Conditions are favorable for fracture growth

vertically upwards and may easily connect with each other. The second factor proposed is geomechanical characterization of the reservoir. According to the study of stress state using Mohr's circle, overpressure in the Marcellus Shale increases the chance of activation of pre-existing fractures especially for the lower value of least principal stress, and it may maintain some fractures in certain dip angle open, although some of them are in non-active state. Unconfined compressive strength (UCS) may be a choice to estimate rock strength in overpressure strata. The result calculated from empirical equations indicates that the Marcellus Shale has significantly lower rock strength than the underlying Onondaga Limestone. Rock strength of the Mahantango is higher than the Marcellus and increases upwards. The difference of rock strength between the Marcellus and Mahantango is not great, which may cause hydraulic fractures to propagate upwards.

Acknowledgements

This research is funded through the U.S.DOE National Energy Technology Lab part of their Marcellus Shale Energy and Environmental Laboratory (MSEEL) (DOE Award No.: DE-FE0024297). We appreciate Northeast Natural Energy LLC. for providing data and technical support.

References

Anderson, E. M. 1951. *The dynamics of faulting and dyke formation with applications to Britain*: Hafner Pub. Co.

Bowers, G. L. 1995. Pore pressure estimation from velocity data: Accounting for overpressure mechanisms besides undercompaction. *SPE Drilling & Completion* **10** (02): 89-95.

Byerlee, J. 1978. Friction of rocks. In *Rock friction and earthquake prediction*, 615-626. Springer.

Eaton, B. A. 1975. The equation for geopressure prediction from well logs. Proc., Fall meeting of the Society of Petroleum Engineers of AIME.

Fjar, E., Holt, R. M., Raaen, A., Risnes, R., and Horsrud, P. 2008. *Petroleum related rock mechanics*, Vol. **53**: Elsevier.

Hottmann, C. and Johnson, R. 1965. Estimation of formation pressures from log-derived shale properties. *Journal of Petroleum Technology* **17** (06): 717-722.

Jarvie, D. M., Hill, R. J., Ruble, T. E., and Pollastro, R. M. 2007. Unconventional shale-gas systems: The Mississippian Barnett Shale of north-central Texas as one model for thermogenic shale-gas assessment. *AAPG bulletin* **91** (4): 475-499.

Rickman, R., Mullen, M. J., Petre, J. E., Grieser, W. V., and Kundert, D. 2008. A practical use of shale petrophysics for stimulation design optimization: All shale plays are not clones of the Barnett Shale. Proc., SPE Annual Technical Conference and Exhibition.

Slotnick, M. 1936. On seismic computations, with applications, I. *Geophysics* **1** (1): 9-22.

Wang, F. P. and Gale, J. F. 2009. Screening criteria for shale-gas systems. Gulf Coast Assoc. *Geol Soc Trans* **59**: 779-793.

Wilson, T. H., Carr, T., Carney, B., Yates, M., MacPhail, K., Morales, A., Costello, I., Hewitt, J., Jordon, E., and Uschner, N. 2018. Marcellus Shale model stimulation tests and microseismic response yield insights into mechanical properties and the reservoir discrete fracture network. *Interpretation* **6** (2): T231-T243.

Zoback, M. D. 2010. *Reservoir Geomechanics*: Cambridge University Press.